Temperature Control of Heterogeneous Reactive Distillation

Shih-Ger Huang, Chien-Lin Kuo, and Shih-Bo Hung
Dept. of Chemical Engineering, National Taiwan University of Science and Technology, Taipei 106-07, Taiwan

Yi-Wei Chen and Cheng-Ching Yu
Dept. of Chemical Engineering, National Taiwan University, Taipei 106-17, Taiwan

DOI 10.1002/aic.10247
Published online in Wiley InterScience (www.interscience.wiley.com).

In this work, we explore the temperature control of heterogeneous reactive distillation. By heterogeneous reactive distillation, we mean a two-liquid phase exists in the reflux drum and a decanter is used to separate the aqueous product from the organic reflux. Process characteristics of n-butyl propionate are explored and a systematic procedure is proposed for the design of butyl propionate reactive distillation. The control structure design procedure consists of the following steps: (1) setting the control objective, (2) selection of manipulated variables, (3) determination of temperature-control trays, (4) finding controller settings for regulatory control, and (5) providing feedforward compensation for production rate variation. Because specifications on the bottoms product have to be met and stoichiometric balance has to be maintained, we have a 2 × 2 control problem with two obvious inputs: reboiler duty and feed ratio. The reactive distillation exhibits unique temperature sensitivities and the nonsquare relative gain successfully identifies temperature-control trays, which results in an almost one-way decoupled system. Therefore, decentralized PI controllers are used at the regulatory level. As a result of the unique feature of a kinetically controlled distillation column, maintaining constant tray temperatures does not imply the same quality specification. Feedforward temperature compensation is necessary to maintain the desired product composition. The proposed design procedure is further extended to butyl acetate reactive distillation, where a similar process behavior is observed, and good control performance can be achieved using simple temperature control. © 2004 American Institute of Chemical Engineers *AIChE J,* 50: 2203–2216, 2004

Keywords: esterification, n-butyl propionate, n-butyl acetate, reactive distillation, heterogeneous distillation, temperature control

Introduction

Reactive distillation provides an attractive alternative for process intensification, especially for reaction/separation systems with reversible reactions. The literature on reactive distillation has grown rapidly in recent years and the book by Doherty and Malone (2001) provides an updated summary. However, relatively few reports discuss process control aspects of reactive distillation columns. These are reviewed in a recent report by Al-Arfaj and Luyben (2000). Al-Arfaj and Luyben (2000, 2002a,b) proposed several control structures for different types of reversible reactions (A + B ↔ C + D, A + B ↔ C, and A ↔ B + C) and consecutive reactions for the product C and by-product D (A + B → C and A + C → D). They showed that (1) reaction stoichiometric balance is crucial for a

Correspondence concerning this article should be addressed to C.-C. Yu at ccyu@ntu.edu.tw.

system with multiple reactants and (2) a simple control strategy works satisfactorily for these complex dynamics.

Similar to the gradual replacement of methyl *tert*-butyl ether (MTBE) with ethyl *tert*-butyl ether (ETBE) (Sneesby et al., 1997), this work is a continuous effort to study the production of less-volatile solvents to replace light solvents such as methyl acetate or ethyl acetate. In this work, we explore the esterification of propionic acid and *n*-butanol to form *n*-butyl propionate (Lee et al., 2002; Liu and Tan, 2001). *n*-Butyl propionate has increasingly been used as a cleaning solvent for processing polymers because of its relatively low volatility. The process falls into a specific class of reactive distillations: heterogeneous reactive distillation (or three-phase reactive distillation; Chiang et al., 2002). By heterogeneous reactive distillation, we mean a two-liquid phase exists in the reflux drum and a decanter is used to separate the aqueous product from the organic reflux. Next, we extend the study to the esterification of acetic acetic acid and *n*-butanol to form *n*-butyl acetate (Gangadwala et al., 2003; Hanika et al., 1999; Venimadhavan et al., 1999; Wang et al., 2003) to provide a possible generalization.

The objective of this work is to devise a control structure for the *n*-butyl propionate process and the control objective is to maintain the propionate quality at specification while keeping the acid purity at the ppm (parts per million) level. This would require two on-line analyzers. Instead of using expensive and less-reliable on-line composition analyzers, the temperature control of this type of three-phase reactive distillations is explored.

Heterogeneous Reactive Distillation

By heterogeneous reactive distillation, we mean that a two-liquid phase exists in the reflux drum and a decanter is used to separate the aqueous product from the organic reflux. For esterification reactions, *n*-propyl acetate, butyl acetate, amyl acetate, and butyl propionate are good examples because they all share the following characteristics (Huang and Yu, 2003):

(1) A large two-liquid zone exists

(2) The minimum boiling azeotrope is located in the two-phase zone

(3) One end of all tie lines points to the direction of a pure component (typically water for esterification)

Vapor–liquid–liquid equilibrium and reaction kinetics

n-Butyl propionate typically is synthesized from propionic acid and *n*-butyl alcohol by esterification. However, ternary azeotropes were found in the mixture of *n*-butanol–*n*-butyl acetate–water. This may lead to difficulty in downstream separation when the conventional reactor/separator process is used. Obviously, reaction distillation provides an attractive alternative. The esterification can be expressed as

$$\underset{141^\circ C}{C_2H_5COOH} + \underset{117.7^\circ C}{C_4H_9OH} \underset{k_b}{\overset{k_f}{\leftrightarrow}} \underset{146.8^\circ C}{C_2H_5COOC_4H_9} + \underset{100^\circ C}{H_2O} \quad (1)$$

The normal boiling points (NBP) in Eq. 1 show that the acetate is the highest boiler, the acid is the second highest boiler, whereas water has the lowest NBP. The reaction is catalyzed by acidic cation exchange resin (Amberlyst 35). A quasi-homogeneous model with nonideal-solution assumption (Lee et al., 2002) is used

$$r = k_f a_{\mathrm{HOPr}} a_{\mathrm{BuOH}} + k_r a_{\mathrm{BuOPr}} a_{\mathrm{H_2O}} \quad (2)$$

where r is the reaction rate per unit catalyst weight [mol/(min · kg cat)] and a stands for the activity of corresponding components; k_f is the forward reaction rate constant [mol/(min · kg cat)]

$$k_f = 1.6786 \times 10^{10} e^{-\{7954/[T(K)]\}} \quad (3)$$

with T in Kelvin and the rate constant for the reverse reaction k_r is

$$k_r = 3.1085 \times 10^{8} e^{-\{7135/[T(K)]\}} \quad (4)$$

This is a slightly endothermic reaction with relatively small heat effect and the equilibrium constant is around 7. The catalyst price is assumed to be 40.74 \$/kg and a catalyst life of one year is assumed in this study.

Following Liu and Tan (2001), the nonrandom two-liquid (NRTL) activity coefficient model is used for the vapor–liquid–liquid equilibrium (VLLE) for the quaternary system (Table 1). The Hayden–O'Conell second virial coefficient model with association parameters is used to account for the dimerization of propionate acid in the vapor phase. The Aspen Plus built-in association parameters are used to compute fugacity coefficients.

The quaternary system has three minimum-boiling binary azeotropes (*n*-butanol–water, *n*-butyl propionate–water, and water–propionic acid) and one maximum-boiling binary azeotrope (propionic acid–*n*-butyl propionate). There is one ternary azeotrope for water–butanol–*n*-butyl propionate that corresponds to the lowest boiling azeotropic temperature (92.9°C). Notice that liquid–liquid (LL) envelopes are found in three (Figures 1b–d) out of four ternary subsystems and, moreover, a very large LL envelope (type 2) is observed for the water–butanol–*n*-butyl propionate system (Figure 1c). This corre-

Table 1. Binary Parameters of the NRTL Model for the Propionic Acid (1), *n*-Butyl Alcohol (2), *n*-Butyl Propionate (3), and Water (4) System*

NRTL Equation:

$$\ln \gamma_i = \frac{\sum_{j=1}^{m} \tau_{ji} G_{ji} x_j}{\sum_{k=1}^{m} G_{ki} x_k} + \sum_{j=1}^{m} \frac{x_j G_{ij}}{\sum_{k=1}^{m} G_{kj} x_k} \left[\tau_{ij} - \left(\frac{\sum_{r=1}^{m} x_r \tau_{rj} G_{rj}}{\sum_{k=1}^{m} G_{kj} x_k} \right) \right]$$

$$G_{ij} = \exp(-\alpha_{ij}\tau_{ij}) \qquad G_{ji} = \exp(-\alpha_{ij}\tau_{ji})$$

$$\tau_{ij} = \frac{A_{ij}}{T} \qquad \tau_{ji} = \frac{A_{ji}}{T} \qquad \tau_{ii} = \tau_{jj} = 0$$

(i, j)	A_{ij} (K)	A_{ji} (K)	α_{ij}
(1, 2)	−65.94	260.635	24.8029
(1, 3)	1320.3	−753.07	0.2636
(1, 4)	−94.58	895.58	0.2909
(2, 3)	−108.03	315.78	0.3000
(2, 4)	−366.82	1666.4	0.2000
(3, 4)	772.79	1973.64	0.2970

*Liu and Tan (2001).

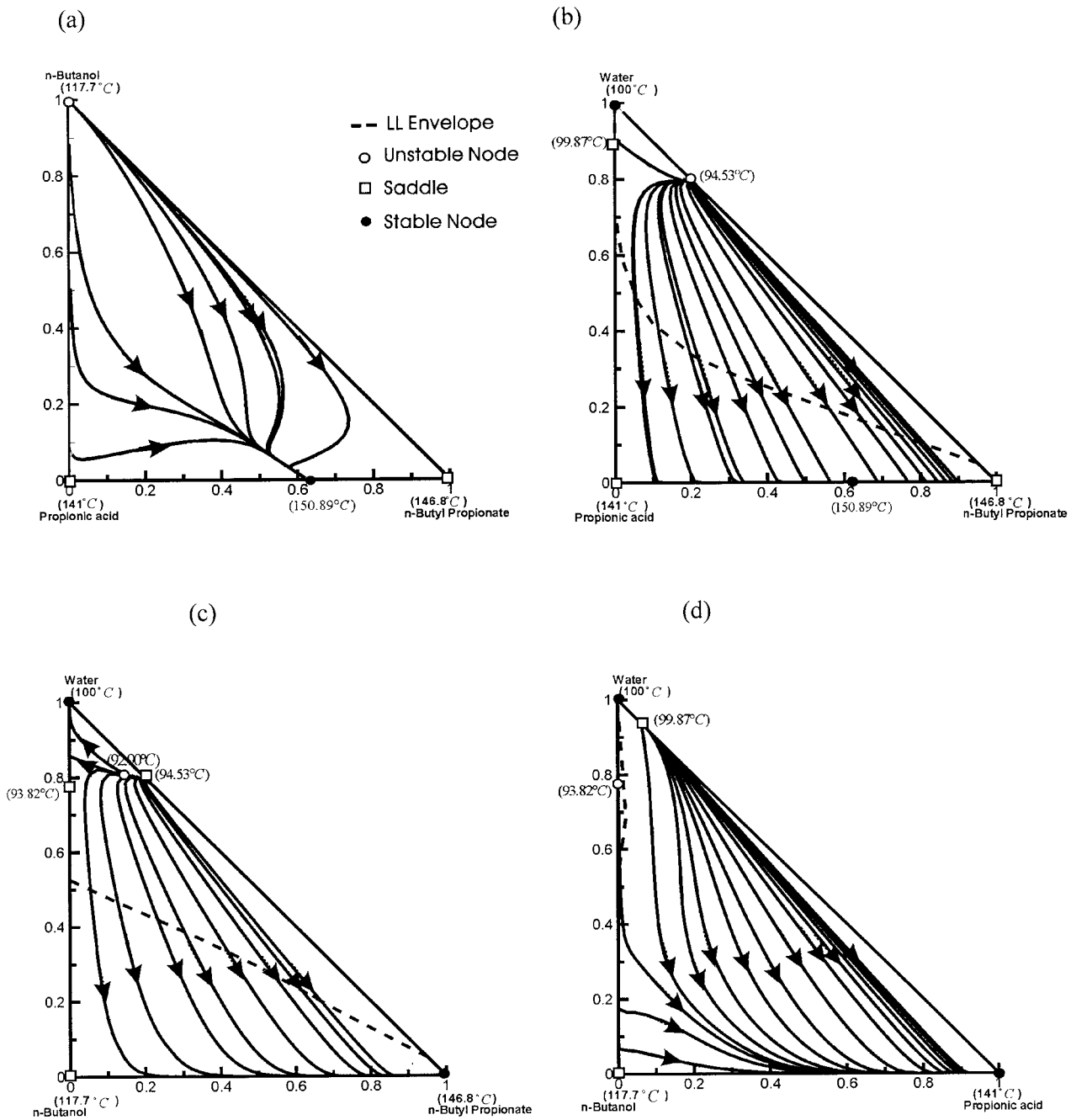

Figure 1. Residue curve maps (RCMs) and LLE envelope for four different ternary combinations.

(a) *n*-butanol–*n*-butyl propionate–propionic acid; (b) water–*n*-butyl propionate–propionic acid; (c) water–*n*-butyl propionate–*n*-butanol; (d) water–propionic acid–*n*-butanol.

sponds to about 50% of the composition space, as shown in Figure 1. The residue curve map (RCM) indicates that, in the acid-free case, the overhead composition of a distillation operation will converge to the ternary azeotrope, which lies within the two-liquid zone. Following the coordinate transformation of Doherty and Malone (2001),

$$X_A = x_{\mathrm{HOPr}} + x_{\mathrm{BuOPr}} \qquad X_B = x_{\mathrm{BuOH}} + x_{\mathrm{BuOPr}} \tag{5}$$

The LL envelope for the quaternary system can be visualized in a 2-D plot. Figure 2 shows that all the tie lines slope toward the pure water end, which implies that a decanter should be installed that will give relatively high-purity water in the aqueous phase.

Steady-state design

A systematic procedure is devised to design heterogeneous reactive distillation. Here, we extend the approach of Chiang et

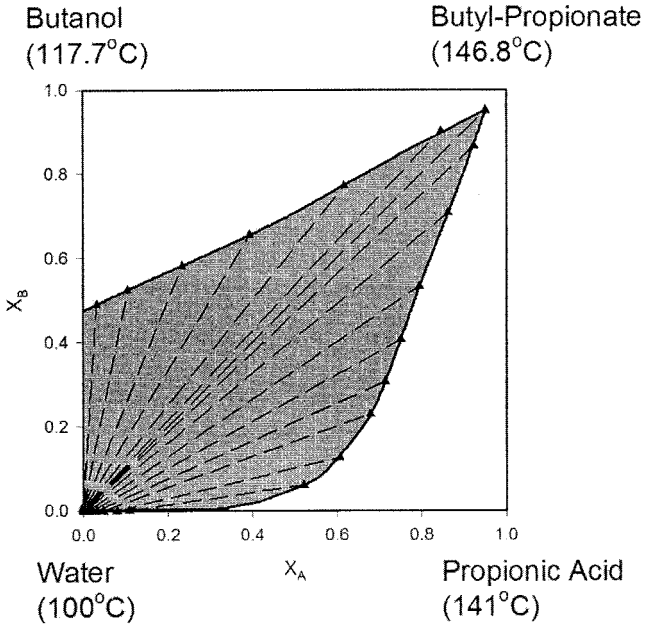

Figure 2. Two-liquid phase and tie lines for the quaternary system.

al. (2002) by rearranging feed tray locations. Initially, the arrangement of feed streams is based on consideration of reaction kinetics, where the heavy reactant (propionic acid) is fed to the top tray of the reactive zone and the light reactant (butanol) enters from the lower section of the reactive zone.

For a system with given specifications on the products and a given production rate, the design steps are (Huang and Yu, 2003) as follows:

(1) Fix a number of reactive trays (N_{Rxn}).

(2) Place the heavy reactant feed on the top tray of the reactive zone and the light reactant feed on the lower section of the reactive section.

(3) Estimate the tray numbers in the rectifying sections (N_R).

(4) Find the minimum number of trays of the stripping section ($N_{S,\min}$) from the short-cut design with a given specification and set $N_S = 2N_{S,\min}$.

(5) Adjust reboiler duty until the bottom product specification (99% *n*-butyl propionate) is met (because organic phase is under total reflux, we have only one degree of freedom).

(6) Go back to step 3 and change the number of trays in the rectifying section (N_R) until the total annual cost (TAC; Chiang et al., 2002) is minimized (because of the type II LLE, practically, we do not have control over water purity).

(7) Go back to step 2 and vary the feed tray locations until TAC is minimized with acceptable acid purity in the bottom (<200 ppm).

(8) Change the number of reactive trays (N_{Rxn}) until the TAC is minimized.

The RADFRAC of Aspen Plus was used to carry out steady-state simulations. The column diameter is sized using a short-cut method (Douglas, 1988), according to the vapor rate and a typical weir height of 5 cm is used. Thus, the available reactor volume for each reactive tray can be computed. Note that Aspen Plus provides better numerical stability using holdup volume–based kinetics, although the kinetic data for these two cases were catalyst weight–based rate constants. Care must be taken to convert the literature rate constants to the holdup-based rate expressions. Provided with catalyst density ($\sim$ 770 kg/m^3) and volume fraction of the total holdup occupied by the catalysts (typically values of 30–50% and 50% is assumed in this work), correct rate constants can be obtained, as shown in the Appendix. The TAC calculation was based on the cost models of Douglas (1988) and Chiang et al. (2002). The optimized design is shown in Figure 3 and Table 2 gives values and costs of the salient parameters. The column has a total of 37 trays, with 6 stripping trays, 25 reactive trays (trays 7–31), and 6 rectifying trays. The optimum feed tray locations are tray 29 (NF1) and tray 31 (NF2). The acid composition in the bottoms is kept to 76 ppm while maintaining propionate purity at 99%. The phase split in the decanter automatically gives a moderately pure water composition (95%).

Figure 4A shows most of the stripping section trying to separate propionate from butanol. The acid is consumed early in the reactive zone and its purity is kept low in the stripping section. A significant reaction is observed between trays 25 and 31, as shown in the thick long-dashed line as the fraction of the total reaction. This type of reaction rate profile is within our expectation because it is necessary to further react the limiting reactant (acid) in trays 7–24 to meet the stringent acid specification in the bottoms. Significant temperature breaks are also observed in the stripping section (trays 2–6) and the rectifying section (trays 35–37), as shown in Figure 4B.

Control

The control objective is to maintain bottoms propionate purity while keeping the acid concentration at a ppm level. Instead of using direct composition control, temperatures are used to infer product composition. This is a multivariable control problem and decentralized PI controllers are used in this work.

Procedure

A typical multivariable control system design procedure consists of the following steps: (1) selection of manipulated variables, (2) determining measurement locations, (3) variable pairing, (4) controller tuning, and (5) feedforward compensation.

Manipulated Inputs. As indicated earlier, the organic-phase condensate is under total reflux and we are left with only one manipulated input, reboiler duty. Another manipulated variable naturally is the feed ratio (Figure 3) for this double-feed column because the feed ratio has to be adjusted to maintain stoichiometric balance (Al-Arfaj and Luyben, 2000).

Temperatures. Before examining measurement selection criteria, let us first examine the sensitivity of temperature profiles as manipulated variables change. As the heat input changes ($\pm$0.5%), two substantial changes are observed (Figure 5). One is in the stripping section, which is typical for conventional distillation, and the other is in the rectifying section as a result of altered reaction rates (compare Figure 4). The latter comes from the effect of increasing (or decreasing) reaction rate, which has not been seen in nonreactive distillation columns. Nonlinear behavior can be seen for a small

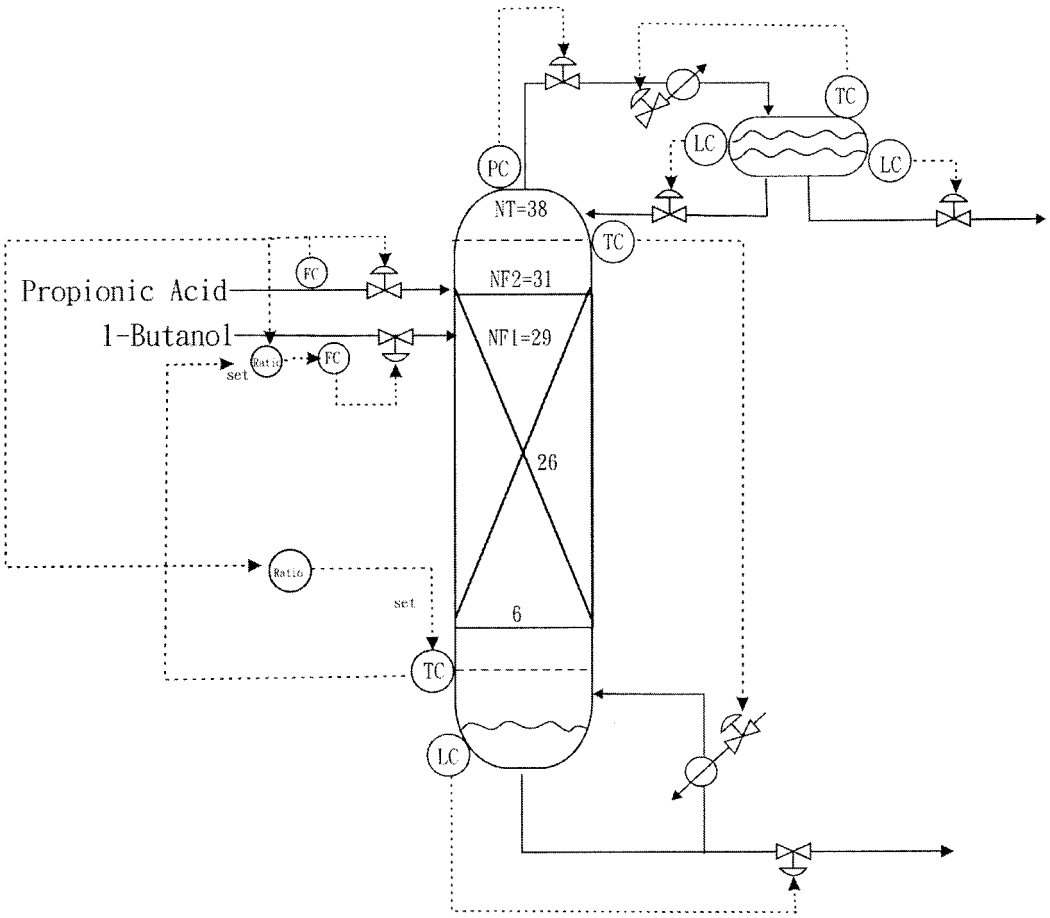

Figure 3. Temperature-control scheme for the butyl propionate reactive distillation.

Feed trays NF1 (tray 29) and NF2 (tray 31); reactive trays 9–31; temperature-control trays T_3 and T_{36}.

change in the feed ratio, as shown in Figure 5. A larger and wider temperature deviation is observed when acid is present in excess. The asymmetry in Figure 5 comes from the fact that the excess acid activates the reaction capability in trays 7–24 and a significant amount of propionate (heaviest component) is produced and, subsequently, results in a much greater increase in temperature. Note that this is not the result of temperature control. Similar behavior can be observed if we choose to use direct composition control: the real reason is that we deliberately design the column asymmetrically (to maintain a trace amount of acid in the bottoms).

Table 3 shows the steady-state gain matrix (**K**) between the temperatures and two inputs (Q_R and $F_{\text{butanol}}/F_{\text{acid}}$). The nonsquare relative gain (NRG) of Chang and Yu (1990) is used for measurement selection

$$\Lambda^N = \mathbf{K} \otimes (\mathbf{K}^+)^T \tag{6}$$

Here, Λ^N stands for the NRG; $\otimes$ denotes element-by-element multiplication; and the superscripts T and $+$ correspond to transpose and pseudo-inverse, respectively. From the definition, the temperatures with a large row sum imply that the temperature profile is best maintained by holding these two temperatures constant. Table 4 shows the distribution of row sums throughout the column and the results indicate two sections in the column with significant row sums, one in the stripping section and the other in the rectifying section (indicated by arrows). The largest ones in each group were selected as the temperature-control trays: trays 3 and 36 (T_3 and T_{36}), as shown in Table 4. These two temperatures correspond to the locations with large temperature breaks (Figure 4).

Pairing. Here, we have a 2×2 multivariable system. The relative gain array (RGA) is used for input–output pairing. For this temperature-controlled reactive distillation, the RGA is

$$\Lambda = \begin{array}{c} \begin{matrix} Q_R & F_{\text{butanol}}/F_{\text{acid}} \end{matrix} \\ \begin{bmatrix} 1.0217 & -0.0217 \\ -0.0217 & 1.0217 \end{bmatrix} \end{array} \begin{matrix} T_{36} \\ T_3 \end{matrix} \tag{7}$$

We have a system with RGA almost equal to 1. Actually, Figure 5 already reveals that this is a one-way decoupled system (that is, T_{36} is not sensitive to feed ratio change). Therefore, the controller structure becomes: pair T_{36} with reboiler duty and pair T_3 with feed ratio.

Tuning for Temperature Loops. Once the control structure is set, decentralized PI controllers are automatically tuned. First, the ultimate gain and ultimate period are identified using sequential relay feedback of Shen and Yu (1994) and, then, PI controller settings are obtained following the Tyreus–Luyben tuning rule.

Table 2. Steady-State Parameters for Butyl Propionate Reactive Distillation

Total no. of trays (N_T)	37
Stripping (N_s)/reactive (N_{rxn})/rectifying (N_R)	6/25/6
Propionic acid feed tray (NF2)	31
n-Butanol feed tray (NF1)	29
n-Butanol feed flow rate (kmol/h)	50
Propionic acid feed flow rate (kmol/h)	50
Top product flow rate (kmol/h)	51.1
Bottoms product flow rate (kmol/h)	48.9
Distillate	
Propionic acid (mole fraction)	0.0286
n-Butanol (mole fraction)	0.0195
n-Butyl propionate (mole fraction)	0.0014
Water (mole fraction)	0.9503
Bottoms	
Propionic acid (ppm)	76.2
n-Butanol (mole fraction)	0.0095
n-Butyl propionate (mole fraction)	0.9903
Water (mole fraction)	$<10^{-9}$
Heat duty	
Condenser (GJ/h)	6.23
Reboiler (GJ/h)	4.28
Column diameter (m)	1.355
Heat exchanger area (m^2)	
Condenser	232.18
Reboiler	48.805
Capital cost ($1000)	
Column	445.70
Trays	38.7
Heat exchangers	177.1
Operating cost ($1000)	
Catalyst	96.0
Energy	185.02
Total annual cost ($1000)	525.46

Feedforward Compensation. Normally, for an equilibrium-stage column, the temperature and composition profiles are independent of the feed rate, as long as the quality specifications (or reflux and boilup ratios) are the same. Such invariance, however, is not valid for a kinetically controlled reactive distillation, given that the residence time in the reactive section changes as the production rate varies. Note that a similar scenario is observed in the design of a plantwide control system for a reactor/separator recycle process (Cheng and Yu, 2003; Luyben et al., 1999). Some types of compensations, such as changing recycle flow rate, varying reactor temperature, and manipulating reactor pressure (for gas-phase reactor), must be installed to handle production rate changes. Similarly, compensation must be considered for this kinetically controlled reactive distillation column when temperatures are used to infer product quality. Three possible approaches can be taken to compensate for production rate variation: (1) adjusting the temperature set point, (2) varying the column pressure, and (3) ratioing the feed to the manipulated variable (such as heat duty). The first approach is taken because it lies within the temperature-control framework.

The temperature program can be generated from either steady-state or dynamic simulation (finding the temperature set points while keeping the bottom product composition at specification). In this work, the temperature compensation is obtained from dynamic simulation while keeping the bottom acetate composition at set point. The results show that a linear relationship can be established between one temperature set point and the production rate (T_3 and ΔF in Figure 6). Moreover, the desired product specification can be obtained by compensating for only one temperature set point.

Results

Temperature Control (without Feedforward Compensation). Figure 7 shows that good temperature control can be achieved using simple PI controllers. For ± 10 and $\pm 20\%$ production rate increases, in both cases T_3 and T_{36} return to their set points in less than 50 min. However, butyl propionate composition deviates from its specification because we are controlling temperatures while the acid concentration shows only slight changes. Figure 7 also shows significant nonlinearity and the responses (such as T_3 and feed ratio loop) become oscillatory for a 20% feed rate decrease. For $\pm 5\%$ measurement errors in the feed ratio, good control performance can also be obtained, but asymmetric responses are observed for positive and negative changes, as shown in Figure 8. The reason was indicated

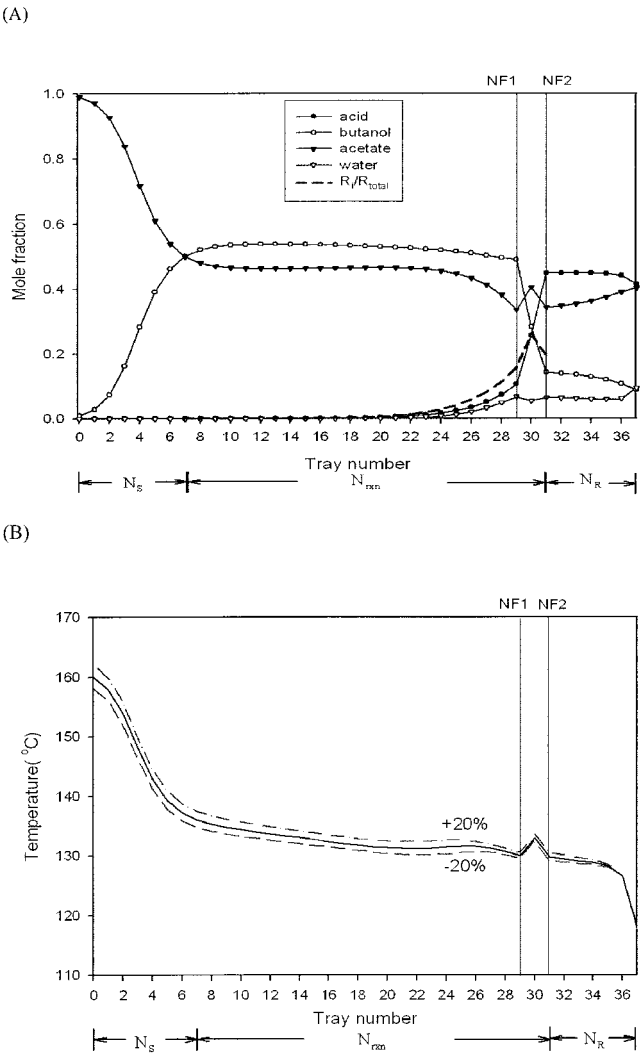

Figure 4. Composition profile and fractions of the total reaction on each reactive tray (A) and nominal temperature profile (solid) and temperature profiles using feedforward temperature control for ±20% feed flow disturbances (B).

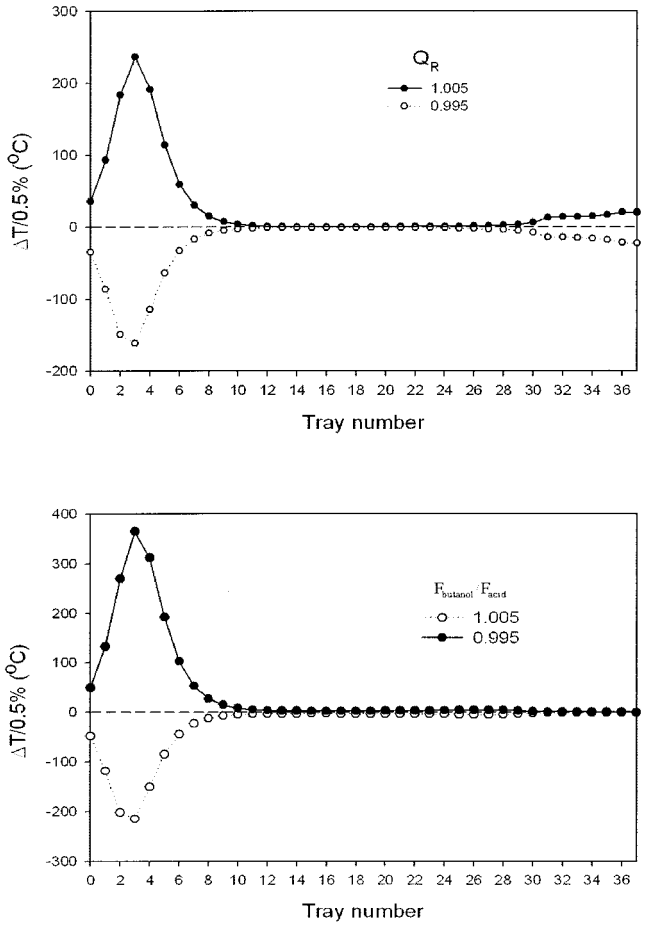

Figure 5. Temperature deviations for ±0.5% changes in reboiler duty (Q_R) (top) and feed ratio (F_{BuOH}/F_{HOPr}) (bottom).

earlier and it can be expected from the temperature sensitivity plots in Figure 5.

Feedforward Compensation. Figure 7 reveals a common problem associated with temperature control: product purity is no longer on spec. For feed ratio disturbance, little steady-state offset is observed; for 20% feed rate disturbance, however, steady-state offsets in the range of 0.2–0.3% can be seen from Figure 7. Because the throughput manipulator is the acid feed flow, a feedforward compensation is devised by adjusting temperature set points of T_3, as shown in Figures 3 and 6. Simulation results in Figure 9 clearly show that it is effective to eliminate offset in product purity while maintaining a similar speed of response. Also note that the acid impurity is still maintained at the acceptable level (<200 ppm).

Extension

To provide possible generalization, the temperature-control approach is extended to another three-phase reactive distillation: butyl acetate esterification.

Butyl acetate process characteristics

n-Butyl acetate is another commonly used heavy solvent and it is synthesized from the esterification of acetic acid and *n*-butyl alcohol. Recently, Veinmadhavan et al. (1999) studied batch reactive distillation policy, Hanika et al. (1999) studied butyl acetate esterification in a pilot-scale system, Gangadwala et al. (2003) provided reaction kinetics using ion-exchange resins as catalysts, and Wang et al. (2003) studied composition control of a butyl acetate reactive distillation column. The reaction can be expressed as

$$\underset{118.1^\circ C}{CH_3COOH} + \underset{117.7^\circ C}{C_4H_9OH} \underset{k_b}{\overset{k_f}{\leftrightarrow}} \underset{126.2^\circ C}{CH_3COOC_4H_9} + \underset{100^\circ C}{H_2O} \qquad (8)$$

The order of normal boiling points (NBPs) follows that of butyl propionate esterification, where the acetate is the highest boiler (126°C) and the acid is the second highest boiler (118.1°C), followed closely by butanol (117.7°C). The vapor–liquid–liquid equilibria (UNIQUAC parameters) were taken from Venimadhavan et al. (1999) and kinetic data were obtained from ion-exchange resin–catalyzed experiments (Gangadwala et al., 2003). A pseudo-homogeneous model, with nonideal-solution assumption (Gangadwala et al., 2003), is adapted here

Table 3. Steady-State Gain Matrix of Butyl Propionate Reactive Distillation

$$\mathbf{K} = \begin{bmatrix} 2.1498 & -0.002064 \\ 2.1294 & -0.0065735 \\ 1.7592 & -0.008668 \\ 1.5751 & -0.009906 \\ 1.4723 & -0.010691 \\ 1.4077 & -0.011162 \\ 1.3654 & -0.011429 \\ 0.70767 & -0.018194 \\ 0.4337 & -0.035951 \\ 0.35351 & -0.045949 \\ 0.25297 & -0.049647 \\ 0.17677 & -0.048278 \\ 0.13214 & -0.044468 \\ 0.11002 & -0.040126 \\ 0.09872 & -0.036232 \\ 0.09 & -0.033131 \\ 0.080515 & -0.030822 \\ 0.070495 & -0.029174 \\ 0.06143 & -0.02803 \\ 0.05447 & -0.027274 \\ 0.05009 & -0.026841 \\ 0.04847 & -0.026738 \\ 0.050155 & -0.02707 \\ 0.056785 & -0.028123 \\ 0.072305 & -0.030531 \\ 0.10516 & -0.035614 \\ 0.17293 & -0.046103 \\ 0.31164 & -0.067584 \\ 0.59471 & -0.11143 \\ 1.1707 & -0.20065 \\ 2.3349 & -0.38079 \\ 4.6421 & -0.73616 \\ 8.924 & -1.3855 \\ 15.318 & -2.3119 \\ 19.933 & -2.8975 \\ 16.6790 & -2.3579 \\ 8.9882 & -1.2574 \\ 3.5320 & -0.4928 \end{bmatrix}$$

Table 4. NRG and Row Sum for Butyl Propionate Reactive Distillation

Tray No.	NRG			
	Q	$F1/F2$	$rs(i)$	
37	0.2133	−0.0014	0.2119	
36	0.2062	−0.0043	0.2019	←
35	0.1390	−0.0047	0.1343	
34	0.1103	−0.0047	0.1056	
33	0.0957	−0.0047	0.0910	
32	0.0871	−0.0047	0.0824	
31	0.0817	−0.0047	0.0770	
30	0.0192	−0.0034	0.0158	
29	0.0038	−0.0021	0.0017	
28	0.0006	−0.0005	0.0002	
27	−0.0010	0.0015	0.0004	
26	−0.0013	0.0024	0.0012	
25	−0.0011	0.0025	0.0015	
24	−0.0008	0.0022	0.0013	
23	−0.0007	0.0018	0.0011	
22	−0.0006	0.0015	0.0009	
21	−0.0005	0.0013	0.0008	
20	−0.0004	0.0012	0.0008	
19	−0.0004	0.0012	0.0008	
18	−0.0003	0.0012	0.0008	
17	−0.0003	0.0012	0.0009	
16	−0.0003	0.0012	0.0009	
15	−0.0003	0.0012	0.0009	
14	−0.0004	0.0012	0.0009	
13	−0.0005	0.0014	0.0009	
12	−0.0007	0.0016	0.0009	
11	−0.0011	0.0022	0.0010	
10	−0.0022	0.0034	0.0012	
9	−0.0046	0.0064	0.0018	
8	−0.0109	0.0145	0.0036	
7	−0.0290	0.0384	0.0094	
6	−0.0839	0.1137	0.0298	
5	−0.2258	0.3202	0.0944	
4	−0.3425	0.5777	0.2352	
3	0.1220	0.2314	0.3534	←
2	0.4384	−0.1900	0.2483	
1	0.1651	−0.0915	0.0737	
0	0.0270	−0.0155	0.0115	

$$r = k_f a_{\mathrm{HOAc}} a_{\mathrm{BuOH}} - k_r a_{\mathrm{BuOAc}} a_{\mathrm{H_2O}} \tag{9}$$

where r is the reaction rate per unit catalyst weight [mol/(s · kg cat)] and a_i represents the activity of corresponding components. k_f is the forward reaction rate constant [mol/(s · kg cat)]

$$k_f = 3.3856 \times 10^6 e^{-\{8499/[T(K)]\}} \tag{10}$$

with T in Kelvin and the rate constant for the reverse reaction k_r is

$$k_r = 1.0135 \times 10^6 e^{-\{8930/[T(K)]\}} \tag{11}$$

This is a slightly exothermic reaction with relatively small heat effect and the equilibrium constant is around 10.

Figure 10 shows that the quaternary system has three minimum-boiling binary azeotropes (*n*-butanol–water, *n*-butyl acetate–water, and *n*-butanol–*n*-butyl acetate) and one maximum-boiling binary azeotrope (*n*-butanol–acetic acid). There are two ternary azeotropes (Figure 10) where the water–butanol–*n*-butyl acetate ternary azeotrope corresponds to the lowest boiling azeotropic temperature (90.7°C). Also note that a very large LL envelope (type 2) is observed for the water–butanol–*n*-butyl acetate ternary system and the lowest boiling azeotrope is located inside the two-liquid zone. Moreover, one end of the tie lines is connected to very high purity water. The VLLE behavior clearly indicates that this esterification system fits the description of a heterogeneous reactive distillation.

Design

For a given production rate of 50 kmol/h, the composition specification for the butyl acetate process is 99% of acetate with a stringent limitation on acid impurity, less than 50 ppm. The process flowsheet consists of a reactive distillation column with a decanter, where the organic phase is totally refluxed and high-purity water is withdrawn from the top as a result of a phase split, as shown in Figure 11. Following the design procedure described earlier, Table 5 gives steady-state operating parameters, as well as associated costs (TAC = $611,620). The column has a total of 34 trays, with 5 stripping trays, 23

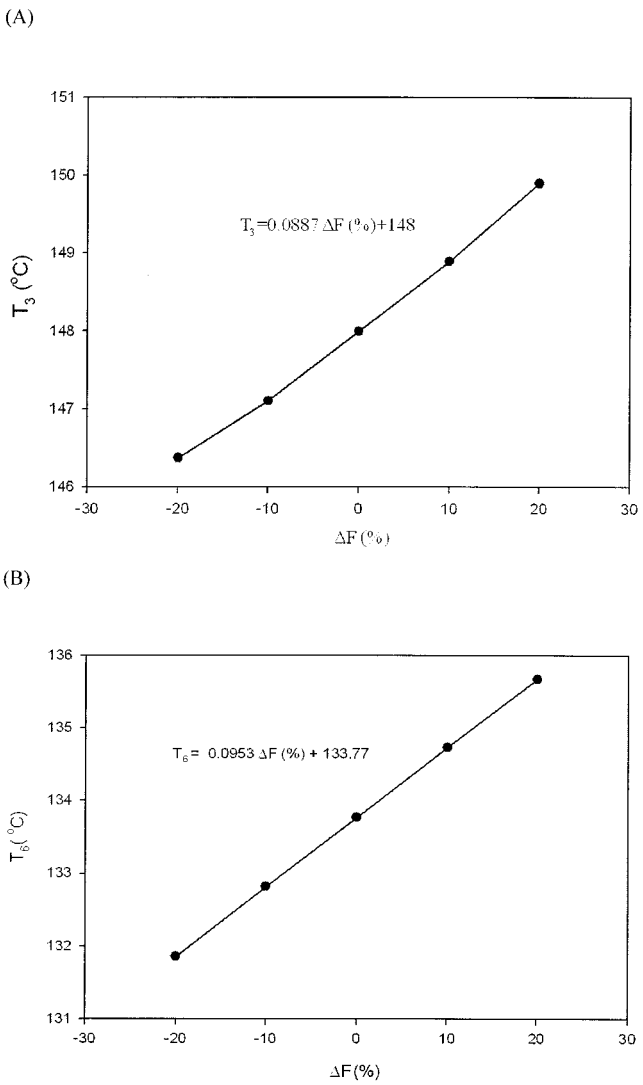

Figure 6. Desired temperature set points under feed flow disturbances for (A) butyl propionate system and (B) butyl acetate system.

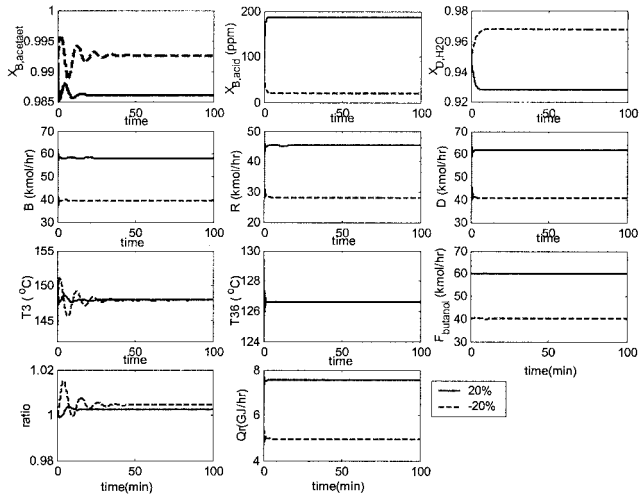

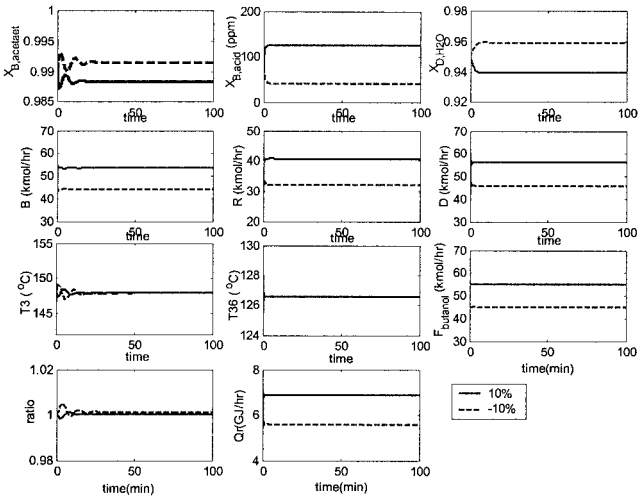

Figure 7. T_3 and T_{36} temperature control for ±10% (top) and ±20% (bottom) feed flow disturbances with feedforward compensation.

reactive trays (trays 6–28), and 6 rectifying trays (trays 29–34). The optimum feed tray locations are tray 26 (NF1 for butanol) and tray 28 (NF2 for acetic acid). The acid composition in the bottoms is kept to 49 ppm while maintaining acetate purity at 99%. The phase split in the decanter automatically gives rather pure water (97.7%). Figure 12A shows that most of the stripping trays perform separation between acetate and butanol. Similar to the butyl propionate case, the acid (the second highest boiler) is consumed early in the reactive zone and its composition is kept low in the stripping section. A significant reaction is observed on trays 23–28, as shown in the thick long-dashed line as the fraction of the total reaction on each reactive tray. It can also be seen that, to meet stringent acid specification in the bottoms, acid is further reacted down the reactive zone to tray 6. The temperature profile basically follows the composition shape of the butyl acetate in the stripping and reactive sections because the only major components are acetate and butanol (Figure 12). A significant temperature break is observed in the reactive zone (trays 23–28)

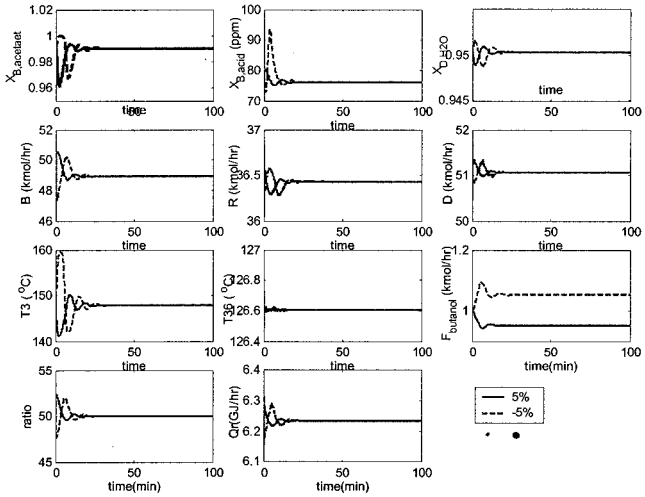

Figure 8. T_3 and T_{36} temperature control for ±5% feed ratio (F_{BuOH}/F_{HOPr}) errors.

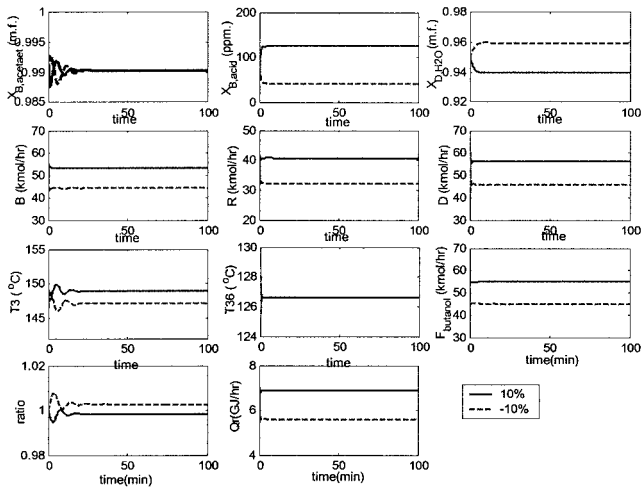

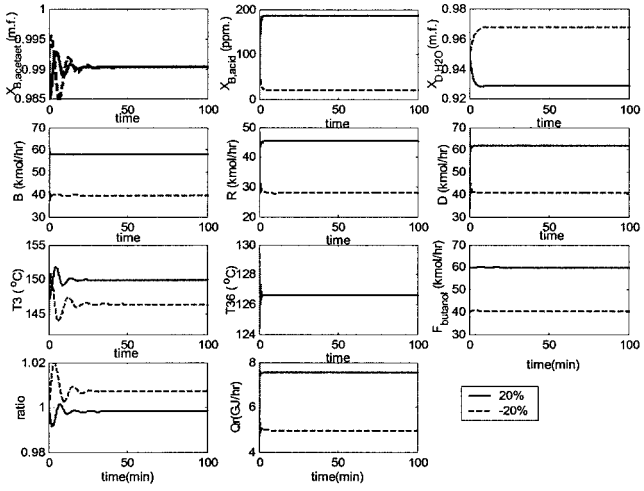

Figure 9. T_3 and T_{36} temperature control with feedforward temperature set point compensation for ±10% (top) and ±20% (bottom) feed flow disturbances.

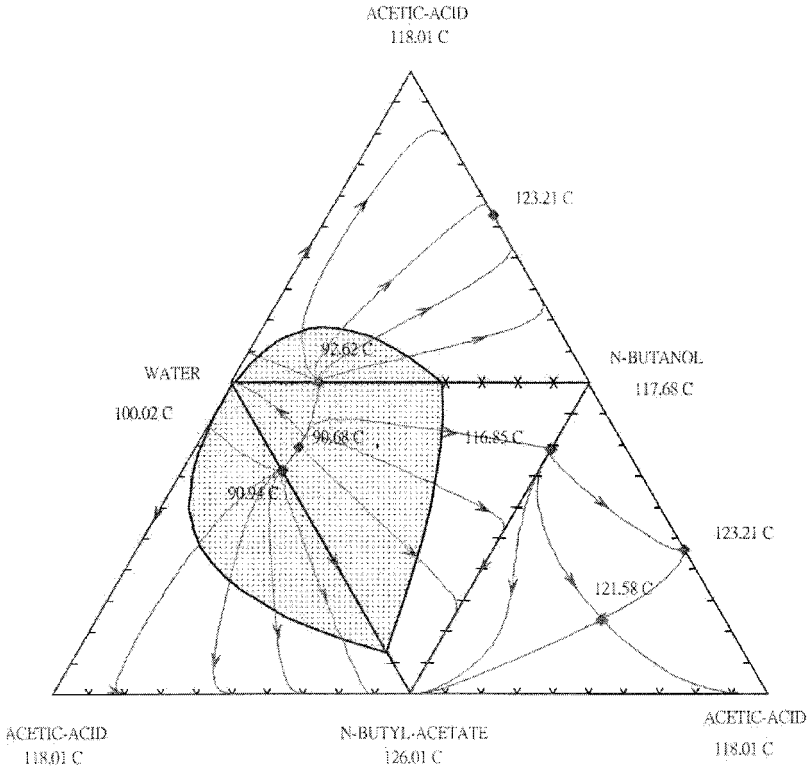

Figure 10. RCMs and LLE envelope for four different ternary combinations (*n*-butanol–*n*-butyl acetate–acetic acid; water–*n*-butyl acetate–acetic acid; water–*n*-butyl acetate–*n*-butanol; water–acetic acid–*n*-butanol), all four binary azeotropes, and two ternary azeotropes are also shown in solid diamonds.

and a mild temperature break can also be seen in the stripping section (trays 6–8), as shown in Figure 12B.

In summary, these two reactive distillation columns, butyl acetate and butyl propionate, share qualitatively similar VLLE

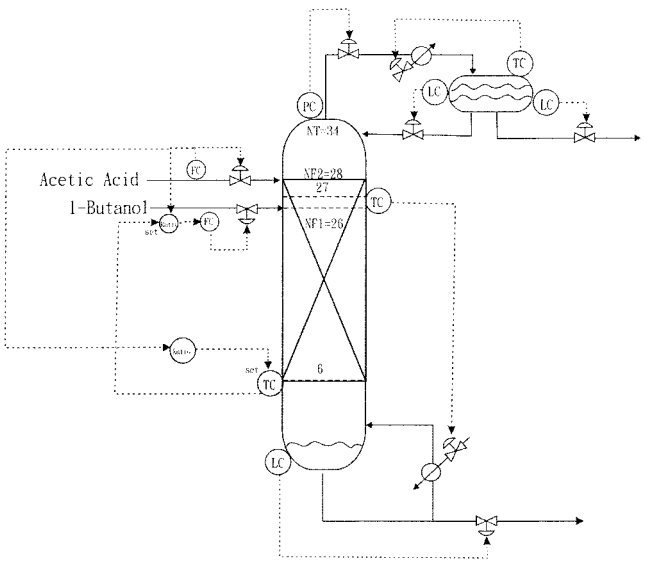

Figure 11. Temperature-control scheme for the butyl acetate reactive distillation.

Feed trays NF1 (tray 26) and NF2 (tray 28), reactive trays 6–28, temperature-control trays T_3 and T_{27}.

Table 5. Steady-State Parameters for Butyl Acetate Reactive Distillation

Total no. of trays (N_T)	34
Stripping (N_s)/reactive (N_{rxn})/rectifying (N_R)	5/23/6
Acetic acid feed tray (NF2)	28
n-Butanol feed tray (NF1)	26
n-Butanol feed flow rate (kmol/h)	50.0
Acetic acid feed flow rate (kmol/h)	50.0
Top product flow rate (kmol/h)	50.4
Bottoms product flow rate (kmol/h)	49.6
Distillate	
Acetic acid (mole fraction)	0.016
n-Butanol (mole fraction)	0.006
n-Butyl acetate (mole fraction)	0.000773
Water (mole fraction)	0.977
Bottoms	
Acetic acid (ppm)	49
n-Butanol (mole fraction)	0.0100
n-Butyl acetate (mole fraction)	0.9900
Water (mole fraction)	$<10^{-9}$
Heat duty	
Condenser (GJ/h)	7.641
Reboiler (GJ/h)	8.885
Column diameter (m)	1.68
Heat exchanger area (m^2)	
Condenser	414.54
Reboiler	69.55
Capital cost ($1000)	
Column	533.20
Trays	51.10
Heat exchangers	219.6
Operating cost ($1000)	
Catalyst	54.60
Energy	265.13
Total annual cost ($1000)	611.62

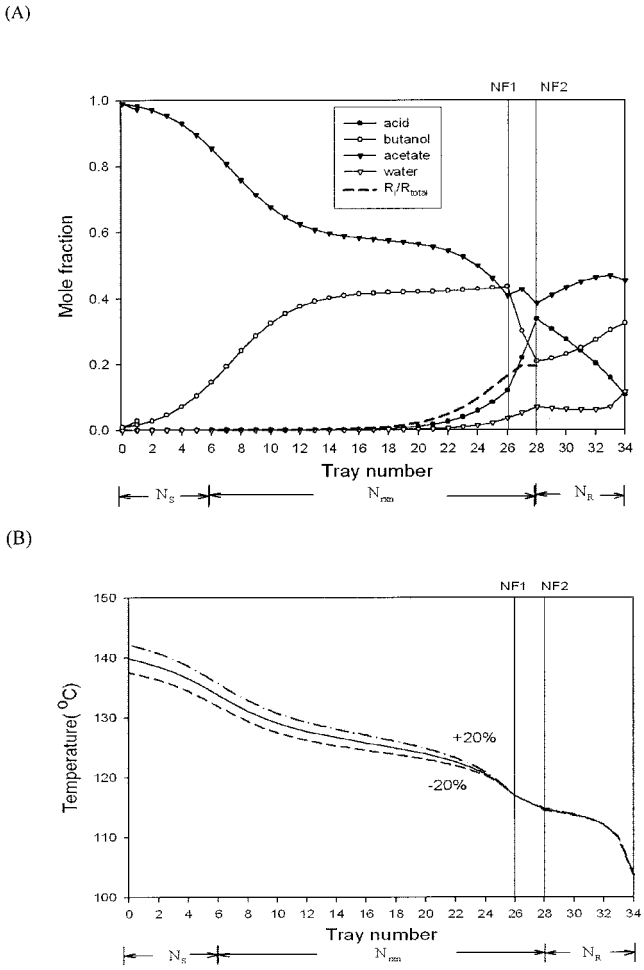

Figure 12. Composition profile and fractions of the total reaction on each reactive tray (A) and nominal temperature profile (solid) and temperature profiles using feedforward temperature control for ±20% feed flow disturbances (B).

and process characteristics. A quantitative difference in the reaction rate, relative volatilities (that is, NBP differences), lead to a slight variation in the tray numbers in the reactive zone, stripping zone, and rectifying zone and in the feed tray locations.

Control

The control objective is to maintain bottoms acetate purity while keeping the acid concentration at a ppm level. Again, multivariable temperature control is used and two manipulated variables are the reboiler duty and feed ratio.

Control Structure. The sensitivity of temperature profiles as manipulated variables change is examined next. As the heat input changes by ±1%, two large deviations are observed (Figure 13). One is in the stripping section, which is typical for conventional distillation, and another is in the reactive zone where significant variations in the reaction rate occur. Again, nonlinear behavior is also observed for a small change in the feed ratio, as shown in the bottom graph of Figure 13. A larger and wider temperature deviation is observed when acid is present in excess ($F_{butanol}/F_{acid}$ = 0.99). The asymmetry in Figure 13 comes from the stringent specification on acid impurity and the reactive trays 23–28 produce excess acetate whenever acid is in excess and, subsequently, results in a much greater increase in temperature. From the temperature profiles, it is expected that the control structure design will be quite similar to that of the propionate system.

Table 6 shows the steady-state gain matrix (**K**) between the temperatures and two inputs (Q_R and $F_{butanol}/F_{acid}$). The nonsquare relative gain (NRG) is given in Table 7. From the row sum of NRG, temperatures on trays 6 and 27 (T_6 and T_{27}) are selected as temperature-control trays (indicated by arrows). These two temperatures correspond to the locations either with large temperature breaks (Figure 12) or having high sensitivity (Figure 13). T_6 is located at the junction of the stripping section and the reactive zone and T_{27} is at the position where the largest fraction of total reaction occurs (Figure 12).

For this 2 × 2 multivariable system, the relative gain array (RGA) is used for input–output pairing. For this temperature-controlled reactive distillation, the RGA is

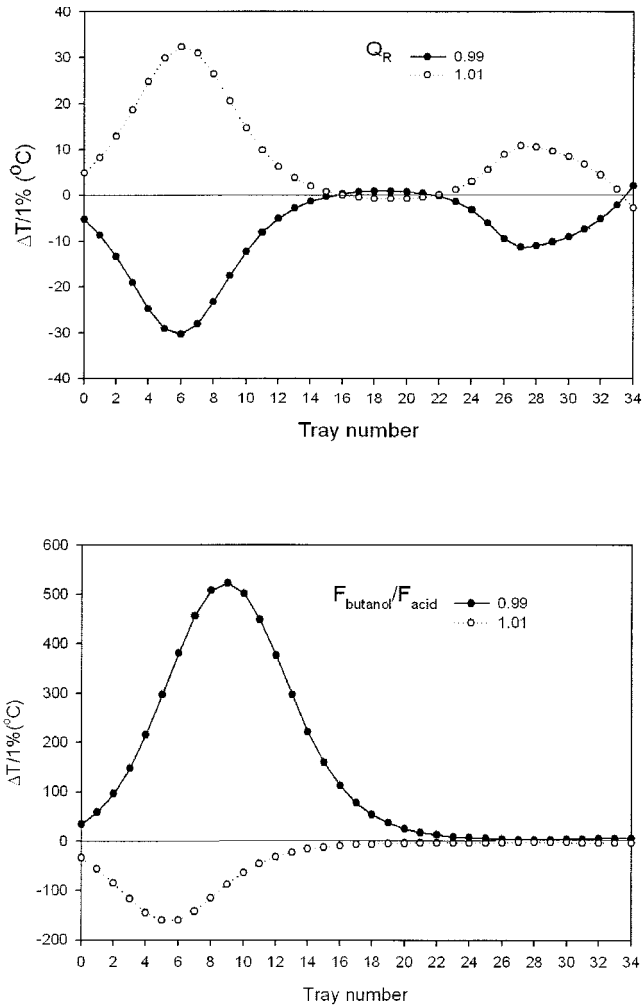

Figure 13. Temperature deviations for ±1% changes in reboiler duty (Q_R) (top) and feed ratio (F_{BuOH})/ (F_{HOAc}) (bottom).

Table 6. Steady-State Gain Matrix of Butyl Acetate Reactive Distillation

$$\mathbf{K} = \begin{bmatrix} -0.24144 & -0.497105 \\ 0.17338 & -0.503725 \\ 0.478625 & -0.422445 \\ 0.70592 & -0.350985 \\ 0.873845 & -0.300595 \\ 0.993605 & -0.267115 \\ 1.076565 & -0.24446 \\ 1.10801 & -0.28633 \\ 0.919325 & -0.34088 \\ 0.583115 & -0.4015 \\ 0.30746 & -0.4896 \\ 0.12732 & -0.61685 \\ 0.01852 & -0.80352 \\ -0.04413 & -1.07908 \\ -0.07664 & -1.48633 \\ -0.087735 & -2.087075 \\ -0.081245 & -2.96857 \\ -0.057385 & -4.24809 \\ -0.013165 & -6.07293 \\ 0.057935 & -8.59482 \\ 0.166625 & -11.909045 \\ 0.3287 & -15.95276 \\ 0.565285 & -20.41266 \\ 0.900435 & -24.736285 \\ 1.35134 & -28.283825 \\ 1.90581 & -30.51889 \\ 2.490035 & -31.106935 \\ 2.95609 & -29.920395 \\ 3.135885 & -27.049175 \\ 2.95176 & -22.854895 \\ 2.477815 & -17.97625 \\ 1.88029 & -13.159135 \\ 1.30989 & -8.9924 \\ 0.846185 & -5.747765 \\ 0.505375 & -3.41318 \end{bmatrix}$$

$$\Lambda = \begin{array}{c} \begin{matrix} Q_R & F_{\text{butanol}}/F_{\text{acid}} \end{matrix} \\ \begin{bmatrix} 1.031 & -0.031 \\ -0.031 & 1.031 \end{bmatrix} \end{array} \begin{matrix} T_{27} \\ T_6 \end{matrix} \qquad (12)$$

Again, this is an almost a one-way decoupled system (that is, T_{27} is not sensitive to feed ratio change). Therefore, decentralized PI controllers are preferred and the controller structure becomes: pair T_{27} with reboiler duty and pair T_6 with feed ratio.

Once the control structure is set, decentralized PI controllers are tuned using a relay feedback autotuner. First, the ultimate gain and ultimate period are identified using sequential relay feedback of Shen and Yu (1994) and, then, PI controller settings are obtained following the Tyreus–Luyben tuning rule. Again, the temperature compensation is obtained from dynamic simulation while keeping the bottom acetate composition at set point. The results show that a linear function can be established between one of the temperature set points and the production rate (T_6 and ΔF in Figure 6). Figure 11 gives the control configuration for the butyl acetate reactive distillation column.

Results. Figure 14 shows that good temperature control can be achieved for ±10% feed flow disturbances. For 20% production rate increase, T_6 and T_{27} return to their set points in less than 20 min. For the −20% feed rate change, however, oscillatory responses are observed (similar to the butyl propionate case; Figure 7) and T_6 did not settle after 100 min. The reason is quite obvious that this overdesigned column leads to overproduction of acetate and, subsequently, to significant distortion in the temperature profile, especially in the lower part of the column (where most of the acetate settles). The feedforward compensated temperature control, on the other hand, promotes substantially improved dynamical responses while keeping acetate on the set point, as shown in Figure 15. The temperatures and composition settle in less than 50 min and asymmetrical behavior is less obvious for the compensated temperature-control scheme. For ±5% measurement errors in feed ratio, good control performance can also be obtained, but asymmetric responses are observed for positive and negative changes, as shown in Figure 16. The reason was indicated earlier and it can be expected from the temperature sensitivity in Figure 13. However, good composition control on acetate can be achieved using the proposed temperature-control scheme.

Conclusion

In this work, vapor–liquid–liquid equilibrium behavior of *n*-butyl propionate, a low volatility solvent, is explored and a

Table 7. NRG and Row Sum for Butyl Acetate Reactive Distillation

	NRG			
Tray No.	Q	$F1/F2$	$rs(i)$	
34	0.0041	0.0007	0.0047	
33	0.0014	−0.0003	0.0011	
32	0.0128	−0.0009	0.0120	
31	0.0288	−0.0011	0.0277	
30	0.0446	−0.0012	0.0435	
29	0.0581	−0.0012	0.0569	
28	0.0684	−0.0012	0.0672	
27	0.0723	−0.0014	0.0708	←
26	0.0493	−0.0014	0.0479	
25	0.0193	−0.0010	0.0183	
24	0.0050	−0.0006	0.0044	
23	0.0006	−0.0002	0.0004	
22	0.0000	0.0003	0.0002	
21	0.0003	0.0008	0.0011	
20	0.0009	0.0016	0.0025	
19	0.0013	0.0030	0.0044	
18	0.0015	0.0055	0.0071	
17	0.0013	0.0102	0.0115	
16	0.0004	0.0189	0.0193	
15	−0.0021	0.0348	0.0326	
14	−0.0076	0.0619	0.0544	
13	−0.0179	0.1033	0.0855	
12	−0.0345	0.1555	0.1210	
11	−0.0549	0.2035	0.1487	
10	−0.0680	0.2238	0.1558	
9	−0.0523	0.1970	0.1448	
8	0.0123	0.1255	0.1378	
7	0.1136	0.0381	0.1517	
6	0.1963	−0.0272	0.1691	←
5	0.2097	−0.0515	0.1582	
4	0.1617	−0.0449	0.1168	
3	0.0973	−0.0281	0.0692	
2	0.0483	−0.0142	0.0341	
1	0.0204	−0.0060	0.0144	
0	0.0073	−0.0022	0.0051	

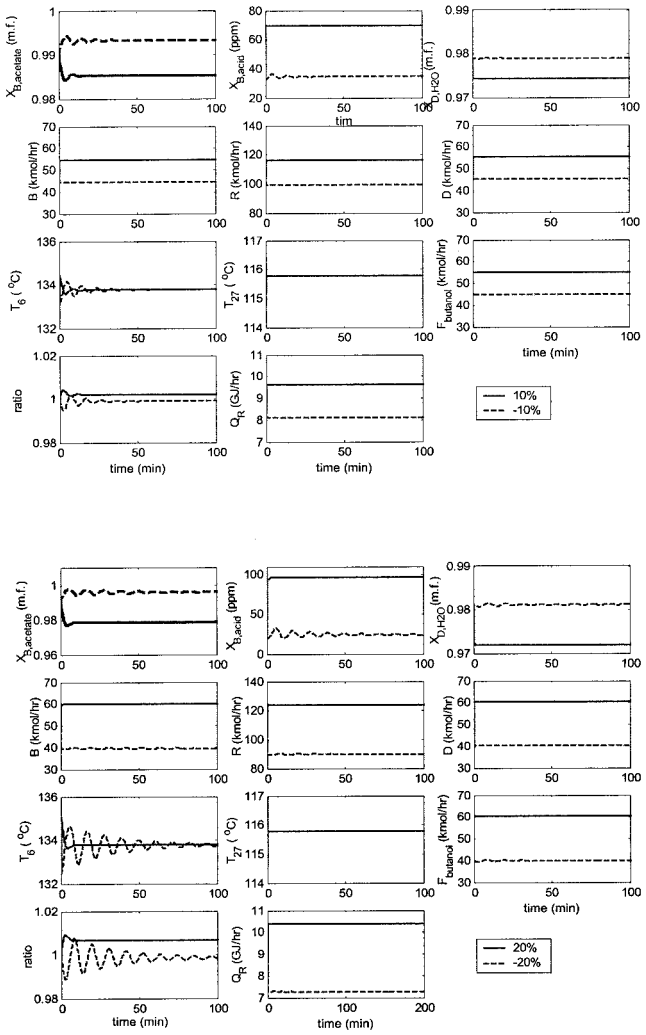

Figure 14. T_6 and T_{27} temperature control for ±10% (top) and for ±20% (bottom) feed flow disturbances without feedforward temperature compensation.

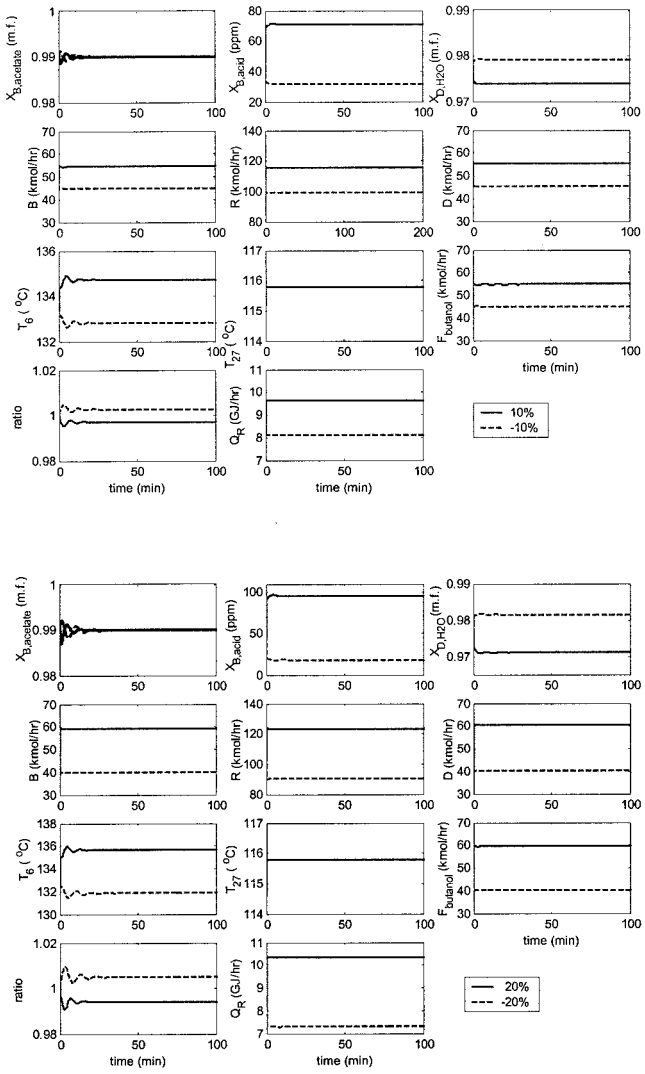

Figure 15. T_6 and T_{27} temperature control with feedforward temperature set point compensation for ±10 and ±20% feed flow disturbances.

systematic procedure is proposed for the design and temperature control of the heterogeneous reactive distillation. A significant two-phase zone and a ternary minimum boiling azeotrope lead to a unique separation characteristic. Next, the issue control structure design for heterogeneous reactive distillation is studied. Because two specifications on the bottoms product (propionate purity and ppm level of acid impurity) have to be met and stochiometric balance needs to be maintained, we have a 2 × 2 control problem with two inputs: heat duty and feed ratio. The reactive distillation exhibits unique temperature sensitivities, compared to those of conventional distillation, and the nonsquare relative gain (NRG) successfully identifies temperature-control trays, which results in an almost one-way decoupled system. Therefore, decentralized PI controllers are used. As a result of the unique feature of kinetically controlled distillation column, maintaining constant tray temperatures does not imply the same quality specification. Feedforward temperature compensation is necessary to maintain the desired product composition. Simulation results show the feedforward

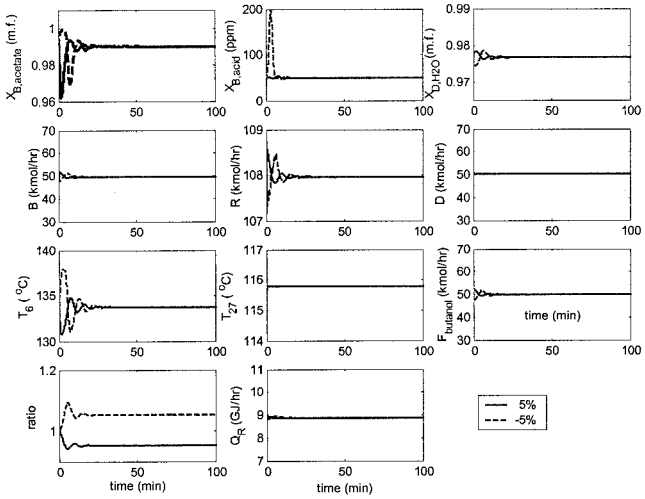

Figure 16. T_6 and T_{27} temperature control for ±5% feed ratio (F_{BuOH}/F_{HOAc}) disturbances.

compensated temperature control not only eliminates steady-state offset in the product quality, but also provides improved transient responses. Finally, to provide possible generalization, the proposed design procedure is extended to butyl acetate reactive distillation (another heavy solvent) and the results show that similar VLLE behavior is observed and similar process configuration is designed. Above all, good control performance can be achieved using simple temperature control.

Acknowledgments

We thank an anonymous reviewer who pointed out the fundamental difference between conventional distillation, equilibrium reactive distillation column, and kinetically controlled reactive distillation. This work was supported by the China Petroleum Corporation of Taiwan under Grant NSC88-CPC-E011-017 and the Ministry of Economic Affairs under Grant 92-EC-17-A-09-S1-019.

Literature Cited

Agreda, V. H., L. R. Partin, and W. H. Heise, "High Purity Methyl Acetate via Reactive Distillation," *Chem. Eng. Prog.*, **86**(2), 40 (1990).

Al-Arfaj, M. A., and W. L. Luyben, "Comparison of Alternative Control Structures for Ideal Two-Product Reactive Distillation Column," *Ind. Eng. Chem. Res.*, **39**, 3298 (2000).

Al-Arfaj, M. A., and W. L. Luyben, "Control of Ethylene Glycol Reactive Distillation Column," *AIChE J.*, **48**, 905 (2002a).

Al-Arfaj, M. A., and W. L. Luyben, "Design and Control of an Olefin Metathesis Reactive Distillation Column," *Chem. Eng. Sci.*, **57**, 715 (2002b).

Aspen Technology, *Aspen Plus User's Manual 10.2*, Aspen Technology, Inc., Cambridge, MA (2000).

Chang, D. M., C.-C. Yu, and I. L. Chien, "Coordinated Control of Blending Systems," *IEEE Trans. Control Syst. Technol.*, **6**, 495 (1998).

Chang, J. W., and C.-C. Yu, "The Relative Gain for Non-Square Multivariable System," *Chem Eng Sci.*, **45**, 1309 (1990).

Cheng, Y. C., and C.-C. Yu, "Effects of Design on Recycle Dynamics and Implications on Control Structure Selection," *Ind. Eng. Chem. Res.*, **42**, 4348 (2003).

Chiang, S. F., C. L. Kuo, C.-C. Yu, and D. S. H. Wong, "Design Alternatives for the Amyl Acetate Process: Coupled Reactor/Column and Reactive Distillation," *Ind. Eng. Chem. Res.*, **41**, 3233 (2002).

Doherty, M. F., and M. F. Malone, *Conceptual Design of Distillation Systems*, McGraw-Hill, New York (2001).

Douglas, J. M. *Conceptual Process Design*, McGraw-Hill, New York (1988).

Gangadwala, J., S. Mankar, S. Mahajani, A. Kienle, and E. Stein, "Esterification of Acetic Acid with Butanol in the Presence of Ion-Exchange Resins as Catalysts," *Ind. Eng. Chem. Res.*, **42**, 2146 (2003).

Gumus, Z. H., and A. R. Ciric, "Reactive Distillation Column Design with Vapor/Liquid/Liquid Equilibria," *Comput. Chem. Eng. Suppl.*, **21**, s983 (1997).

Hanika, J., J. Kolena, and Q. Smejkal, "Butylacetate via Reactive Distillation—Modeling and Experiment," *Chem. Eng. Sci.*, **54**, 5205 (1999).

Huang, S. G., and C.-C. Yu, "Sensitivity of Thermodynamic Parameter to the Design of Heterogeneous Reactive Distillation: Amyl Acetate Esterification," *J. Chin. Inst. Chem. Eng.*, **34**, 345 (2003).

Lee, M. J., J. Y. Chiu, and H. M. Lin, "Kinetics of Catalytical Esterification of Propionic Acid and *n*-Butanol over Amberlyst 35," *Ind. Eng. Chem. Res.*, **41**, 2882 (2002).

Liu, W. T., and C. S. Tan, "Liquid-Phase Esterification of Propionic Acid with *n*-Butanol," *Ind. Eng. Chem. Res.*, **40**, 3281 (2001).

Luyben, W. L., B. D. Tyreus, and M. L. Luyben, *Plantwide Process Control*, McGraw-Hill, New York (1999).

Malone, M. F., and M. F. Doherty, "Reactive Distillation," *Ind. Eng. Chem. Res.*, **39**, 3953 (2000).

Sneesby, M. G., M. O. Tade, R. Datta, and T. N. Smith, "ETBE Synthesis via Reactive Distillation. 2. Dynamic Simulation and Control Aspects," *Ind. Eng. Chem. Res.*, **36**, 1870 (1997).

Venimadhavan, G., M. F. Malone, and M. F. Doherty, "A Novel Distillate Policy for Batch Reactive Distillation with Application to the Production of Butyl Acetate," *Ind. Eng. Chem. Res.*, **38**, 714 (1999).

Venkataraman, S., W. K. Chan, and J. F. Boston, "Reactive Distillation Using ASPEN Plus," *Chem. Eng. Prog.*, **Aug.**, 45 (1990).

Vora, N., and P. Daoutidis, "Dynamics and Control of Ethyl Acetate Reactive Distillation Column," *Ind. Eng. Chem. Res.*, **40**, 833 (2001).

Wang, S. J., D. S. H. Wong, and E. K. Lee, "Control of a Reactive Distillation Column in the Kinetic Regime for the Synthesis of *n*-Butyl Acetate," *Ind. Eng. Chem. Res.*, **42**, 5182 (2003).

Appendix: Kinetics Data Conversion for Aspen Plus

Aspen Plus gives better numerical stability using holdup volume–based kinetics, but the kinetic data for these two cases were catalyst weight–based rate constants. To convert the catalyst weight–based kinetics data to holdup volume–based rate expression, the following information is required: (1) the catalyst density and (2) volume fraction of the total holdup occupied by the catalysts. For amberlyst type of ion-exchange resins the catalyst density ρ_{cat} ranges from 750 to 800 kg/m^3 and, for a typical tray design, the catalyst occupies typically 30–50% of the liquid holdup volume. In this work, $\rho_{cat} = 770$ kg/m^3 is used and we also assume the catalyst occupies 50% of the holdup volume. We use the butyl propionate example to find the input data for the Aspen Plus. The preexponential factor in Eq. 3 is used to illustrate the unit conversion.

$$\begin{aligned} k_f &= 1.6786 \times 10^{10}\,[\text{mol}/(\text{min}\cdot\text{kg cat})] \times 1/60\ (\text{min/s}) \\ &\quad \times 770\ (\text{kg cat/m}^3\ \text{cat}) \times 0.5\ (\text{m}^3\ \text{cat/m}^3) \\ &= 10.77 \times 10^{10}\,[\text{mol}/(\text{m}^3\cdot\text{s})] \end{aligned} \tag{13}$$

Typically, $k_f = 10.77 \times 10^{10}$ mol/(m^3 · s) is the input data to an Aspen simulator.

Manuscript received Dec. 9, 2002, and revision received Dec. 27, 2003.